JASETUI Vol. 1, No. 1 (2026): pp. (38–48)

Journal of Automotive Science and Engineering Technology
University of Ibadan, JASETUI

print-ISSN: 2587-****
https://journals.ui.edu.ng/index.php/JASETUI
e-ISSN: 2587-****

Evaluation of corrosion resistance of automotive AISI 1055 carbon steel in *jatropha tanjorensis* extract inhibited saline and acidic environments

Itopa G. Akande[1,*], Oluwaferanmi M. Enioluwafe[2], Kunle M. Oluwasegun[3], Daniel O. Nasamu[1], Victor E. Okoruwa[1]
[1]*Department of Automotive Engineering, University of Ibadan, Ibadan, 200005, Nigeria.*
[2]*Department of Mechanical Engineering, University of Ibadan, Ibadan, 200005, Nigeria.*
[3]*Department of Mechanical and Manufacturing Engineering, University of Manitoba, Winnipeg, Canada.*

ARTICLE INFO
Keywords:
AISI 1055 Carbon Steel
Weight Loss
Corrosion Test
Jatropha Tanjorensis
Adsorption Isotherm

ABSTRACT
The growing concerns surrounding corrosion deterioration in the automotive, aerospace, petrochemical and other manufacturing industries, where steel is used, have driven the search for sustainable protective strategies. The AISI 1055 carbon steel is valued for its strength in automotive applications; however, it suffers from corrosion attack over time, prompting the need for eco-friendly protection. This study evaluates the effectiveness of Jatropha tanjorensis (tree spinach) stem extract as a green inhibitor for AISI 1055 carbon steel samples in 1 M hydrochloric acid (HCl) and 3.5% sodium chloride (NaCl). The corrosion behaviour was monitored over 21 days at 3-day intervals, using a gravimetric experiment. The adsorption isotherms of the samples were evaluated. The surface morphology of selected samples via Scanning Electron Microscopy (SEM) equipped with Energy-Dispersive Spectroscopy (EDS) was examined. In HCl, the corrosion rate reduces from 2.491 mm/yr to 0.387 mm/yr, with inhibition efficiency peaking at 93.94%. In NaCl, the corrosion rate reduces from 3.155 mm/yr to 0.166 mm/yr, achieving 100% efficiency. Adsorption in HCl followed the Langmuir model ($R^2 = 0.9997$, Day 3), while NaCl showed strong Langmuir adherence ($R^2 = 0.9998$, Day 3), indicating monolayer dominance. The SEM revealed reduced pitting on the inhibited HCl sample, indicating that the Jatropha tanjorensis stem extract offered a sustainable corrosion protection for the steel.

1.0 Introduction

Corrosion presents a persistent and formidable obstacle to the longevity of AISI 1055 carbon steel, a material prized for its mechanical strength and versatility across applications such as automotive, aerospace, industrial machinery, structural frameworks, and heavy-duty tools [1, 2]. The high carbon content of this alloy makes it exceptional in terms of hardness and wear resistance, making it indispensable in sectors where structural integrity and durability are essential [3, 4]. However, its vulnerability intensifies in aggressive environments, such as hydrochloric acid (HCl) used in industrial descaling or sodium chloride (NaCl) prevalent in marine and coastal settings, leading to progressive degradation that impairs its performance [5]. The economic impact of corrosion is immense. Globally, it exerts an estimated annual cost of $2.5 trillion, which is equivalent to 3–4% of the GDP of industrialised nations [6,7]. In Nigeria, a country with a growing industrial base and extensive coastal infrastructure, corrosion-related losses are substantial, with annual expenditures on repairs and replacements reaching approximately ₦1.3 trillion ($3.2 billion USD), including ₦250 billion ($625 million USD) in the oil and gas sector due to pipeline corrosion in the Niger Delta [8]. These statistics emphasise the urgent need for advanced corrosion mitigation strategies, particularly for steels such as AISI 1055 exposed to simulated 1 M HCl and 1 M NaCl conditions [9,10]. Conventional corrosion control strategies have predominantly utilised synthetic inhibitors like chromates, phosphates, and nitrates that form protective coatings on metal surfaces to impede oxidative processes [11-13] [11–13]. These compounds effectively reduce corrosion rates, yet significant drawbacks increasingly limit their application. Their synthesis involves complex chemical processes that elevate production costs, and their toxicity poses risks to human health and ecosystems, complicating disposal under stringent regulatory oversight [14]. In Nigeria, where over 70% of industrial effluents are discharged into water bodies without adequate treatment [15], the environmental consequences of these chemicals are particularly severe. Globally, over 60% of countries have imposed restrictions on hazardous chemical use, heightening the demand for sustainable alternatives [16]. This regulatory and ecological pressure has driven exploration into natural resources, with plant-derived extracts gaining prominence for their efficacy, renewability, and minimal environmental impact [17].

Among these botanical alternatives is Jatropha tanjorensis, commonly known as Tree Spinach, it emerges as a compelling candidate [18]. Native to tropical regions like West Africa and

[0]*Corresponding author: Itopa G. Akande, aigodwin2015@gmail.com
https://doi.org/**.****/jasetui.2026.0001
Received 7 January 2026; Received in revised form 10 June 2026; Accepted 13 June 2026
Available online 14 June 2026
Copyright 2025 Published by Department of Automotive Engr., UI

abundant in Nigeria, this shrub is rich in phytochemicals such as flavonoids, tannins, saponins, and alkaloids, recognised for their potential anticorrosive properties [19]. Unlike synthetic inhibitors, which incur production costs averaging $500 per ton [20], Jatropha tanjorensis offers a cost-effective alternative, with harvesting and processing expenses estimated at less than $50 per ton in local markets [21]. Projections suggest that adopting plant-based inhibitors could reduce corrosion-related costs by up to 25%, a significant prospect for industries worldwide and in Nigeria, where mitigation expenditures reached ₦1.8 trillion ($4.5 billion USD) in 2022 [22]. The protective capacity of Jatropha tanjorensis is intricately tied to its phytochemical constituents and their interactions with the steel surface. Flavonoids, with oxygen-rich heterocyclic structures, are posited to form coordination complexes with metal ions (e.g., Fe^2 or Fe^3) on the steel, stabilising the surface and reducing its reactivity with corrosive agents like H or Cl [23]. The hydroxyl groups in flavonoids enable hydrogen bonding or electron donation to iron, establishing a barrier that inhibits anodic dissolution [24]. Tannins, characterised by their polyphenolic structure, exhibit a pronounced affinity for iron ions, potentially forming insoluble Fe-tannate complexes via chelation [25]. These complexes deposit as a passivating layer, physically shielding anodic sites where oxidation initiates, with their extensive aromatic framework ensuring broad surface coverage [26]. Saponins, with amphiphilic properties arising from hydrophilic glycosidic and hydrophobic aglycone moieties, enhance film formation by improving surface wettability and stabilising the protective layer through micellar structures [27]. This adaptability is particularly valuable in acidic 1 M HCl, where saponins may mitigate pH-induced instability [28]. Alkaloids, featuring nitrogen-containing heterocyclic rings, contribute electron-donating capabilities, forming coordinate bonds with iron atoms to reinforce the protective film [29]. The synergy among these phytochemicals-flavonoids stabilising, tannins passivating, saponins broadening coverage, and alkaloids enhancing chemical bonding-creates a robust, multifaceted defence against corrosion [30].

The mechanism underpinning this protection is adsorption, through which these organic molecules adhere to the steel surface, obstructing corrosive species [31]. Adsorption occurs via two distinct pathways: physical and chemical. Physical adsorption, mediated by weak van der Waals forces, enables rapid, reversible attachment of phytochemicals, forming an initial shield influenced by molecular size, polarity, and surface charge [32]. Chemical adsorption, involving stronger interactions, typically entails electron donation from heteroatoms (oxygen, nitrogen) in phytochemicals to vacant d-orbitals of iron atoms [33]. For example, tannins chelate with Fe^2/Fe^3 to form stable complexes, while flavonoids donate lone pairs from oxygen, creating covalent-like bonds [34]. The film's structure, whether a uniform monolayer (Langmuir isotherm) or a heterogeneous multilayer (Freundlich model), depends on inhibitor concentration, steel surface morphology, and exposure duration [35]. In 1 M HCl, protonation of phytochemicals may enhance electrostatic attraction to the negatively charged steel surface [36], whereas in 1 M NaCl, chloride ions may compete for adsorption sites, requiring robust chemical bonding for sustained efficacy [37]. Studies indicate that optimal adsorption can achieve surface coverage exceeding 90%, markedly reducing corrosion rates [38]. Botanical precedents such as neem [39], ginger [40], papaya [41], and moringa [42] validate plant-based solutions, yet Jatropha tanjorensis remains underexplored. Its abundance in Nigeria and phytochemical richness position it as a unique contender. Therefore, this study aims to assess Jatropha tanjorensis extract as a corrosion inhibitor for AISI 1055 steel in simulated 1 M HCl and 3.5% NaCl solution over 21 days, at concentrations of 0.5–2.5 g/L using gravimetric experiment.

2.0 Experimental Methods

2.1 Metal specimen and preparations

The carbon steel sheet employed in this investigation has the chemical composition detailed in Table 1. The steel was sectioned into coupons with standardised dimensions of 20 mm × 20 mm × 1mm to ensure uniformity and consistency across all samples, facilitating reliable experimental outcomes. These coupons were subsequently cleaned by degreasing in absolute ethanol, air-dried, weighed, and stored before use.

Table 1: Composition of carbon steel used (wt.%)

Element	Fe	C	Mn	Si	P	S
Composition	98.238	0.54	0.73	0.41	0.035	0.047

2.2 Preparation of Jatropha tanjorensis

The Jatropha tanjorensis plant was sourced from Bodija Market in Oyo State. Rather than utilising the commonly consumed leaves, the stems shown in Figure 1, typically considered waste, were used to investigate their potential. Bioactive compounds were extracted from the stems using 80 mL of ethanol. The stems were first dried and pulverised into a fine powder, then combined with ethanol in a sealed glass container. The mixture was agitated periodically to promote the release of compounds. Following extraction, the solution was filtered through cheesecloth, and the ethanol was evaporated. The resulting extract was stored in a dark, airtight glass container for subsequent use. Solutions of varying concentrations 0.5 g/L, 1.0 g/L, 1.5 g/L, 2.0 g/L, and 2.5 g/L were prepared using 60 mL of 1 M HCl and 3.5% NaCl to assess the extract's effectiveness.

Figure 1: Jatropha tanjorensis stem.

2.3 Gravimetric Experiment Procedure

The gravimetric experiment was conducted using test coupons with dimensions of 20 mm × 20 mm × 1 mm. All tests were carried out in solutions exposed to atmospheric oxygen to simulate conditions conducive to corrosion or chemical reactions over a 21-day period. Every three days, the coupons were retrieved, cleaned by gentle scrubbing with a soft brush, degreased, dried, and reweighed. The weight loss for each coupon was calculated as the difference between its initial and final weights, measured with a pre-calibrated weighing balance. To enhance data accuracy, each experiment was replicated three times, and the average weight loss was recorded. The corrosion rate (CR), inhibition efficiency (IE), and surface coverage (θ) were determined using Equations 1, 2, 3 and 4:

$$\Delta W = W_i - W_f \tag{1}$$

$$CR = \frac{W_i - W_f}{At} \tag{2}$$

$$IE\% = \frac{\omega_0 - \omega_1}{\omega_0} \times 100 \tag{3}$$

$$\theta = \frac{\omega_0 - \omega_1}{\omega_0} \tag{4}$$

Here, W_i and W_f represent the initial and final weights of the metal sample, respectively, and ω_0 and ω_1 denote the weight loss values without and with the inhibitor, respectively. A is the surface area of the coupon, and t is the exposure time.

3.0 Results and Discussion

3.1 Gravimetric Analysis of Jatropha tanjorensis Inhibited AISI 1055 Steel in HCl Media

The gravimetric analysis of Jatropha tanjorensis inhibited AISI 1055 carbon steel in 1 M hydrochloric acid (HCl) over a 21-day immersion period is presented in Figure 2 and Table 2. The results demonstrate the extract's effectiveness in mitigating corrosion compared to the uninhibited control [43]. As shown in Figure 1, the control sample (without inhibitor) exhibited severe corrosion, with

weight loss increasing steadily from 0.33 g by Day 3 to 0.45 g by Day 21. In contrast, the addition of Jatropha tanjorensis extract significantly reduced weight loss in a concentration-dependent manner. For the 0.5 g/L Jatropha tanjorensis extract inclusion, the weight loss decreased to 0.16 g after 21 days. Higher concentrations (1.0 g/L and 1.5 g/L) further suppressed corrosion, yielding losses of 0.14 g and 0.11 g, respectively. The most effective inhibition was observed at concentrations of 2.0 g/L and 2.5 g/L. For the 2.0 g/L Jatropha tanjorensis extract inclusion, the total weight loss was 0.08 g, with minimal initial corrosion (0.02 g by Day 3), and for the 2.5 g/L Jatropha tanjorensis extract inclusion, a lower weight loss (0.07 g) was recorded, with a gradual increase from 0.02 g (Day 3) to 0.07 g (Day 21). Table 2 provides a detailed breakdown of weight loss measurements across all tested concentrations and time intervals. The data corroborate the trends illustrated in Figure 2, confirming that Jatropha tanjorensis acts as an effective green inhibitor, with performance-enhancing effects as concentration rises. These findings suggest that the extract forms a protective layer on the steel surface, significantly retarding HCl-induced corrosion [44].

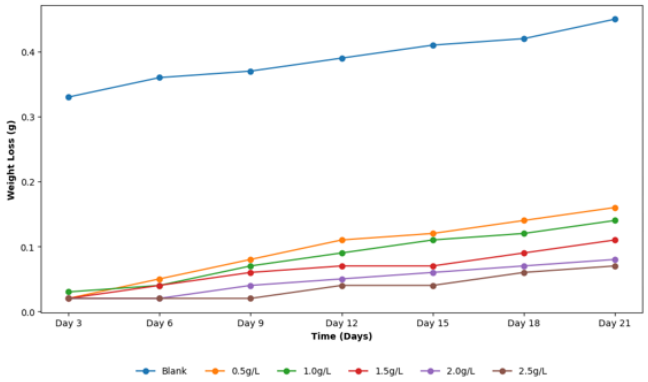

Figure 2: Graph of weight loss against time for uninhibited and inhibited AISI 1055 steel in HCl

The corrosion rates of the carbon steel in hydrochloric acid solutions containing varying concentrations of Jatropha tanjorensis extract is presented in Figure 3 and Table 3. The control sample exhibited characteristic corrosion behaviour, beginning with an initial rate of 12.787 mm/yr at Day 3 before gradually stabilising to 2.491 mm/yr by Day 21. This natural decline reflects the partial passivation that occurs as corrosion products accumulate on the steel surface over time. Introduction of the plant extract dramatically altered the corrosion kinetics. At the lowest tested concentration (0.5 g/L), corrosion rates were immediately reduced to 0.775 mm/yr on Day 3, representing nearly an order of magnitude decrease compared to the uninhibited system. The 1.0 g/L concentration showed comparable initial performance but demonstrated slightly better stability over the 21 days, maintaining rates between 0.775-0.904 mm/yr after Day 9. Intermediate concentrations (1.5 g/L) exhibited further improvement, with corrosion rates consistently remaining below 0.775 mm/yr and showing particularly stable values from Day 12 onward (0.678 - 0.646 mm/yr). The most significant corrosion suppression occurred at higher extract concentrations. The 2.0 g/L treatment achieved corrosion rates as low as 0.443 mm/yr by Day 21, while the 2.5 g/L concentration maintained exceptional stability throughout the testing period, with rates fluctuating minimally between 0.291 - 0.387 mm/yr after Day 12. This remarkable performance suggests the formation of a highly effective and durable protective layer at these concentrations.

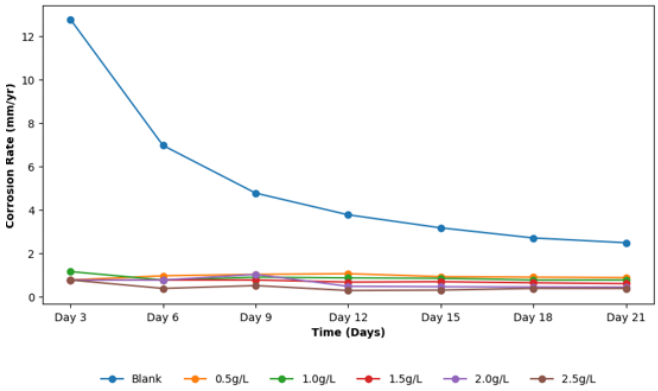

Figure 3: Graph of corrosion rate against time for of AISI 1055 carbon steel in HCl with extract

The inhibition efficiency (I.E.) data presented in Table 4 and Figure 4 reveal important insights into the protective mechanism and stability of Jatropha tanjorensis extract in hydrochloric acid environments. The results demonstrate a clear concentration-dependent relationship in both initial performance and long-term stability of the protective films. At the lowest concentration (0.5 g/L), the extract exhibited excellent initial inhibition (93.94% on Day 3) but declined significantly to 64.43% by Day 21, indicating limited film stability. The 1.0 g/L concentration exhibited similar initial performance (90.91%) with marginally better retention (68.89% at Day 21), suggesting slightly improved film durability. Notably, the 1.5 g/L concentration demonstrated superior film stability, maintaining 75.55% efficiency after 21 days despite starting at the same initial efficiency as lower concentrations. The data reveal a critical performance threshold at 2.0 g/L concentration. While showing comparable initial efficiency (93.94%), this concentration achieved peak performance on Day 12 (87.19%) before stabilizing at 82.22% by Day 21. This pattern suggests the formation of a self-repairing protective layer that reaches optimal coverage after several days of exposure. The 2.5 g/L concentration provided the most stable protection overall, maintaining efficiency above 84% throughout the testing period with minimal fluctuation (93.94 to 84.46%).

All concentrations show their highest efficiency at Day 3, indicating rapid initial adsorption. The rate of efficiency decline slows progressively with increasing concentration. Concentrations 2.0 g/L exhibit characteristic stabilisation after Day 12. The 2.5 g/L curve shows the flattest profile, confirming superior film stability. Table 4 provides additional mechanistic insights. The gradual efficiency improvement seen at 2.0 g/L between Days 9-12 suggests film reorganisation. The consistent high performance at 2.5 g/L indicates near-complete surface coverage. The parallel efficiency trends for 1.5-2.5 g/L after Day 15 imply similar protection mechanisms. The maintenance of >80% efficiency at 2.0-2.5 g/L confirms practical applicability. These results demonstrate that while Jatropha tanjorensis extract provides excellent initial corrosion protection at all concentrations, only formulations 2.0 g/L maintain sufficient efficiency for long-term industrial applications. The extract's ability to form stable protective films at higher concentrations, particularly the 93.94% to 84.46% retention at 2.5 g/L, confirms its potential as a viable green inhibitor for acid cleaning and pickling processes. The concentration-dependent performance patterns suggest the extract operates through a combination of surface coverage and film reinforcement mechanisms that become more effective at higher dosages [45].

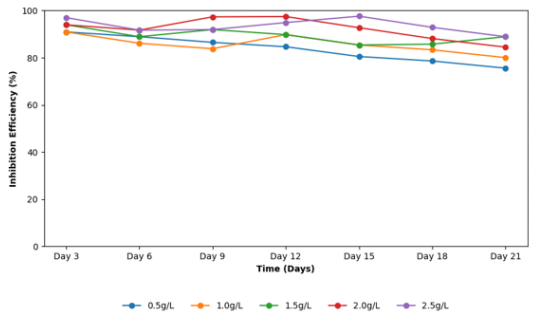

Figure 4: Graph of inhibition efficiency against time for AISI 1055 carbon steel in HCl with extract

3.2 Adsorption isotherm of Jatropha tanjorensis on steel in HCl solution

The Langmuir R^2 values for Jatropha tanjorensis in HCl are consistently high, ranging from 0.9840 to 0.9997 across all days as indicated in Figures 5-11. The values indicate a strong fit to the Langmuir model, confirming that the adsorption of Jatropha tanjorensis onto the steel surface follows monolayer adsorption on a homogeneous surface with fixed active sites. The highest value (0.9997 on Day 3) suggests excellent inhibitor adsorption at the early stage, which remains relatively stable throughout the experiment. The slight decrease on Day 9 (0.9840) may indicate minor desorption or surface saturation effects, but the subsequent rise shows that the inhibitor maintains its effectiveness over time. The consistently high R^2 values suggest that Jatropha tanjorensis adsorption is mainly governed by chemisorption, forming a strong protective layer that limits corrosion. The steadily high R^2 value over time also signifies improved surface interactions between the steel and the extract [46]. The persistent high linearity ($R^2 > 0.98$) and near-unity slopes confirm the stability of the monolayer mechanism in acidic conditions. These findings substantiate the extract's effectiveness as a corrosion inhibitor through the formation of durable surface monolayers, with particular efficacy observed at higher concentrations. The data provide compelling evidence for the extract's potential in industrial applications requiring reliable corrosion protection in acidic media.

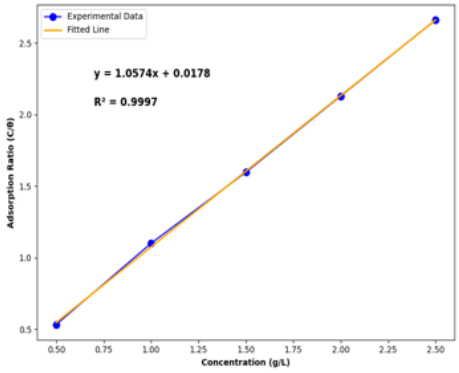

Figure 5: Graph of Langmuir isotherm on Day 3.

3.3 Gravimetric Analysis of Jatropha tanjorensis Inhibited AISI 1055 Steel NaCl Media

The gravimetric analysis of Jatropha tanjorensis as a corrosion inhibitor for AISI 1055 steel in sodium chloride (NaCl) solution over 21 days is indicated in Table 5 and Figure 12. The data reveal a concentration-dependent reduction in corrosion, with the extract demonstrating significant protective effects compared to the uninhibited control. As illustrated in Figure 12, the control sample (without inhibitor) exhibited the highest corrosion rate, with weight loss escalating from 0.43 g on Day 3 to 0.57 g by Day 21. In contrast, the addition of Jatropha tanjorensis extract noticeably suppressed corrosion. For the 0.5 g/L Jatropha tanjorensis inhibited steel, limited protection was provided, with weight loss rising from 0.02 g (Day 3) to 0.14 g (Day 21). The 1.0 g/L and 1.5 g/L Jatropha tanjorensis inclusion provided improved inhibition, restricting final weight losses to 0.06 g and 0.11 g, respectively. A more effective corrosion resistance was achieved at higher concentrations of 2.0 g/L, maintaining strong inhibition, with weight loss ranging narrowly from 0.00 g to 0.09 g over 21 days. The 2.5 g/L Jatropha tanjorensis addition showed the best performance, with negligible weight loss (0.00–0.03 g), confirming the formation of a robust protective film on the steel surface. The results underscore Jatropha tanjorensis's efficacy as a green inhibitor in NaCl environments, with inhibition efficiency scaling with concentration. These findings suggest that the extract's protective mechanism is highly effective in chloride-rich media, particularly at concentrations 2.0 g/L, making it a promising candidate for corrosion mitigation in saline conditions.

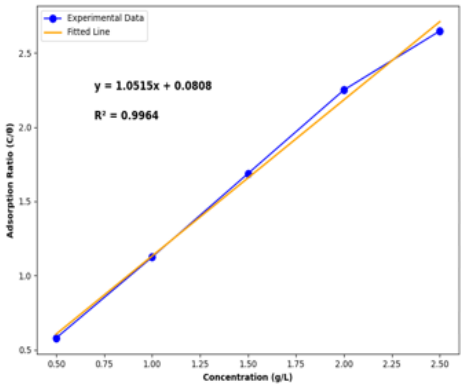

Figure 6: Graph of Langmuir isotherm on Day 6

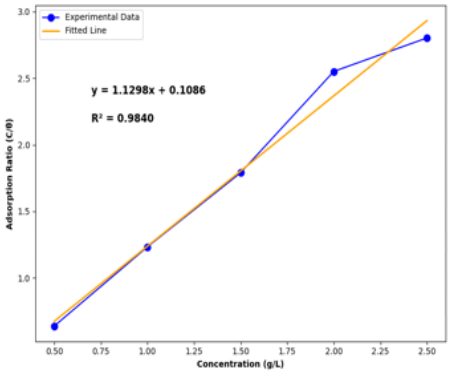

Figure 7: Graph of Langmuir isotherm on Day 9

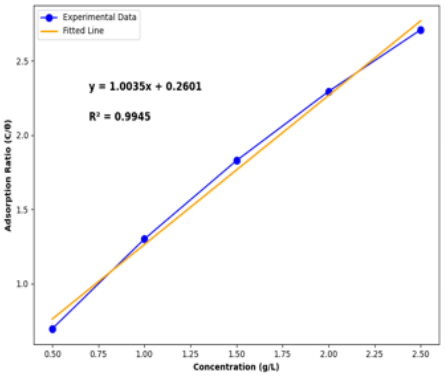

Figure 8: Graph of Langmuir isotherm on Day 12

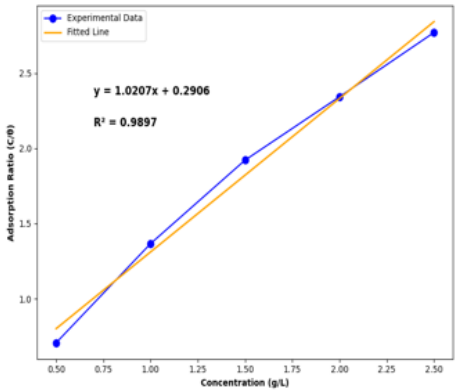

Figure 9: Graph of Langmuir isotherm on Day 15

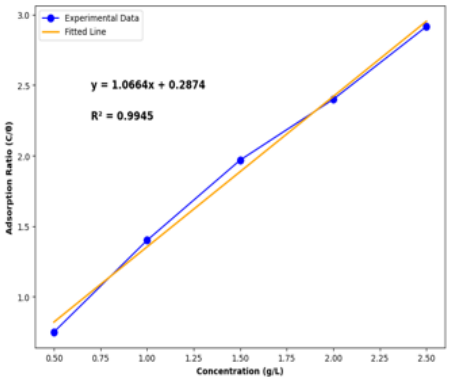

Figure 10: Graph of Langmuir isotherm on Day 18

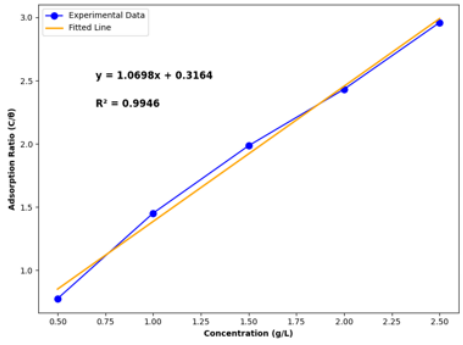

Figure 11: Graph of Langmuir isotherm on Day 21

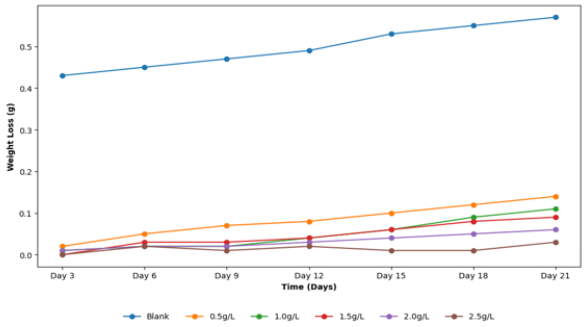

Figure 12: Graph of weight loss against time for uninhibited and inhibited AISI 1055 steel in NaCl

The corrosion protection performance of Jatropha tanjorensis extract in sodium chloride solution is clearly demonstrated in Table 6 and Figure 13. The uninhibited control sample showed characteristically high initial corrosion rates, beginning at 16.661 mm/yr on Day 3 before gradually declining to 3.155 mm/yr by Day 21. This decrease reflects the partial surface passivation that occurs during prolonged exposure to chloride environments, though the persistent corrosion confirms the aggressive nature of NaCl solutions toward carbon steel 47. The addition of Jatropha tanjorensis extract produced dramatic reductions in corrosion rates across all tested concentrations. At the lowest concentration (0.5 g/L), corrosion rates were immediately suppressed to 0.775 mm/yr on Day 3 - representing a reduction compared to the control. While this concentration maintained relatively stable rates around 0.775 mm/yr throughout the testing period, the 1.0 g/L treatment showed superior performance, achieving even lower initial rates of 0.387 mm/yr and maintaining values between 0.258-0.332 mm/yr after Day 6. The extract demonstrated particularly impressive performance at higher concentrations. The 1.5 g/L treatment matched the initial corrosion suppression of 1.0 g/L (0.387 mm/yr on Day 3) and showed excellent stability, with rates remaining below 0.609 mm/yr for the entire 21-day period. Most remarkably, the 2.0 and 2.5 g/L concentrations achieved near-complete corrosion suppression, with initial rates of 0.000 mm/yr on Day 3 and long-term rates never exceeding 0.581 mm/yr and 0.166 mm/yr, respectively.

Several important trends emerge from Figure 13. Initially, all extract-containing systems show substantially lower and more stable corrosion rate profiles compared to the control. Subsequently, the corrosion rate curves become progressively flatter with increasing extract concentration, indicating more effective and durable surface protection. More so, the concentration-dependent performance is particularly evident in the first 9 days of exposure, after which the higher concentrations (1.5 g/L) maintained consistently low corrosion rates. Table 6 further revealed that while all concentrations provided immediate corrosion reduction, the higher concentrations (1.5 g/L) demonstrated superior ability to maintain stable protection throughout the exposure period. The exceptional performance at 2.5 g/L, maintaining corrosion rates below 0.166 mm/yr after Day 12, suggests the formation of an especially robust protective film that effectively resists chloride-induced attack.

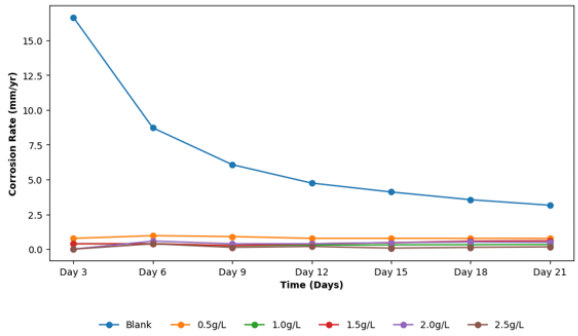

Figure 13: Graph of corrosion rate against time for of AISI 1055 carbon steel in NaCl with extract

The inhibition efficiency performance of Jatropha tanjorensis extract in sodium chloride solution demonstrates clear concentration-dependent behaviour, as evidenced by the data in Table 7 and Figure 14. The extract showed excellent initial protective capabilities across all tested concentrations, with inhibition efficiencies exceeding 90% on Day 3 for every formulation. However, the long-term stability of this protection varied significantly with concentration. At the lowest concentration of 0.5 g/L, the initial 95.35% efficiency gradually declined to 84.22% by Day 21, indicating some breakdown of the protective film over time in the aggressive chloride environment. Moderate concentrations of 1.0 g/L and 1.5 g/L exhibited improved stability compared to the lowest dose, though still showed measurable efficiency losses over the 21-day test period. The 1.0 g/L concentration maintained 89.48% of its initial protection by Day 21, while the 1.5 g/L formulation retained 87.73% efficiency.

Table 2: Weight (W) loss of carbon steel in 1 M HCl with Jatropha tanjorensis extract

Time	W. Loss (g)	W. Loss (g)	W. Loss (g)	W. Loss (g)	W. Loss (g)	W. Loss (g)
DAY 3	0.33	0.02	0.03	0.02	0.02	0.02
DAY 6	0.36	0.05	0.04	0.04	0.02	0.02
DAY 9	0.37	0.08	0.07	0.06	0.04	0.02
DAY 12	0.39	0.11	0.09	0.07	0.05	0.04
DAY 15	0.41	0.12	0.11	0.07	0.06	0.04
DAY 18	0.42	0.14	0.12	0.09	0.07	0.06
DAY 21	0.45	0.16	0.14	0.11	0.08	0.07

Table 3: Corrosion rates of AISI 1055 carbon steel in HCl with Jatropha tanjorensis extract

Time	CR_1	CR_2	CR_3	CR_4	CR_5	CR_6
DAY 3	12.787	0.775	1.162	0.775	0.775	0.775
DAY 6	6.975	0.969	0.775	0.775	0.775	0.387
DAY 9	4.779	1.033	0.904	0.775	1.033	0.517
DAY 12	3.778	1.066	0.872	0.678	0.484	0.291
DAY 15	3.177	0.930	0.852	0.697	0.465	0.310
DAY 18	2.712	0.904	0.775	0.646	0.452	0.387
DAY 21	2.491	0.886	0.775	0.609	0.443	0.387

This gradual decline suggests that while these intermediate concentrations form reasonably stable protective layers, some desorption or film degradation still occurs with prolonged exposure to chloride ions. The most impressive performance was observed at the highest concentrations tested. The 2.0 g/L treatment not only achieved perfect 100% initial inhibition but maintained exceptional protection throughout the exposure period, still showing 96.48% efficiency after 21 days. Even more remarkably, the 2.5 g/L concentration demonstrated near-flawless persistence, with efficiency values consistently above 94% and peaking at 98.10% on Day 15. This outstanding performance indicates the formation of an extremely robust protective barrier that resists breakdown even in challenging chloride conditions. Several important patterns emerge from careful examination of the data.

All concentrations showed their maximum efficiency within the first three days of exposure, confirming the extract's ability to rapidly form protective surface films. Also, the rate of efficiency decline slowed progressively with increasing concentration, demonstrating the dose-dependent nature of film stability. The concentrations at or above 2.0 g/L exhibited remarkably flat efficiency profiles, indicating the formation of particularly durable protective layers. The nearly constant high efficiency maintained by the 2.5 g/L concentration suggests this formulation may represent an optimal balance between inhibitor quantity and protective performance in saline environments.

These results have important practical implications. The extract's ability to maintain greater than 96% inhibition efficiency at 2.5 g/L over three weeks of continuous exposure suggests strong potential for marine and offshore applications where long-term corrosion protection in chloride-rich environments is essential. The concentration-dependent performance characteristics indicate that while lower doses may be suitable for short-term applications, the highest concentrations provide the durability needed for extended service.

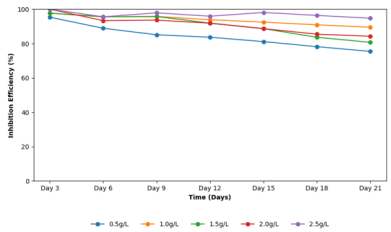

Figure 14: Graph of inhibition efficiency against time for AISI 1055 carbon steel in NaCl with extract

3.4 Adsorption Isotherm of Jatropha tanjorensis on Steel in NaCl Solution

The Langmuir R^2 values for Jatropha tanjorensis in NaCl are also high, ranging from 0.9789 to 0.9998, indicating a strong fit to the Langmuir model. The highest R^2 (0.9998 on Day 3) confirms excellent initial adsorption, similar to its performance in HCl. However, a slight decrease is observed on Days 15 and 18 (0.9812 and 0.9789, respectively), which may be attributed to competitive adsorption between Jatropha tanjorensis molecules and chloride ions (Cl) in NaCl. The values remain high overall, suggesting that Jatropha tanjorensis still follows a monolayer adsorption mechanism in NaCl, though chloride interactions may slightly weaken the protective film over time compared to HCl. The adsorption behavior of Jatropha tanjorensis extract on high-carbon steel in NaCl solution was systematically investigated through Langmuir isotherm analysis, as presented in Figures 15-21.

The results demonstrate a strong adherence to the Langmuir adsorption model, indicating monolayer coverage as the primary mechanism of corrosion inhibition. Initial adsorption measurements (Day 3, Figure 15) showed excellent agreement with the Langmuir model, evidenced by an R^2 value of 0.9998 and the regression equation $y = 0.9855x + 0.03851$. The near-unity slope (0.9855) and minimal positive intercept confirm the formation of a well-ordered monolayer during the early exposure period. This initial behavior represents nearly ideal Langmuir adsorption characteristics. As the exposure period progressed to Days 6-12 (Figures 16-18), the system maintained strong Langmuir conformity with R^2 values ranging from 0.9979 to 0.9991. The slope values remained close to unity (1.005-1.040), while the intercepts showed a gradual increase from 0.02643 to 0.07695.

These observations suggest minor modifications to the adsorption process while retaining the fundamental monolayer mechanism. The latter stages of exposure (Days 15-21, Figures 19-21) revealed slightly reduced but still significant Langmuir linearity, with R^2 values between 0.9789 and 0.9890. The increasing intercept values (0.1273 to 0.1678) and slope variations (1.007-1.042) indicate evolving surface interactions while maintaining monolayer dominance. This temporal evolution suggests dynamic adjustments in the protective layer composition. While minor variations in adsorption parameters occur, the persistent high linearity ($R^2 > 0.97$) confirms the stability of the monolayer mechanism. These findings support the extract's effectiveness as a corrosion inhibitor in chloride-containing environments through the formation of durable surface monolayers. The data particularly highlight the extract's ability to maintain effective adsorption characteristics despite prolonged exposure to aggressive NaCl solution. The initial near-perfect Langmuir behaviour (Day

Table 4: Corrosion rates of AISI 1055 carbon steel in HCl with Jatropha tanjorensis extract

Time	CR_1 (mm/yr)	CR_2 (mm/yr)	CR_3 (mm/yr)	CR_4 (mm/yr)	CR_5 (mm/yr)	CR_6 (mm/yr)
DAY 3	12.787	0.775	1.162	0.775	0.775	0.775
DAY 6	6.975	0.969	0.775	0.775	0.775	0.387
DAY 9	4.779	1.033	0.904	0.775	1.033	0.517
DAY 12	3.778	1.066	0.872	0.678	0.484	0.291
DAY 15	3.177	0.930	0.852	0.697	0.465	0.310
DAY 18	2.712	0.904	0.775	0.646	0.452	0.387
DAY 21	2.491	0.886	0.775	0.609	0.443	0.387

Table 5: Weight loss of AISI 1055 carbon steel in NaCl with Jatropha tanjorensis extracts

Time	WL_1 (g)	WL_2 (g)	WL_3 (g)	WL_4 (g)	WL_5 (g)	WL_6 (g)
DAY 3	0.43	0.02	0.01	0.01	0.00	0.00
DAY 6	0.45	0.05	0.02	0.02	0.03	0.02
DAY 9	0.47	0.07	0.02	0.02	0.03	0.01
DAY 12	0.49	0.08	0.03	0.04	0.04	0.02
DAY 15	0.53	0.10	0.04	0.06	0.06	0.01
DAY 18	0.55	0.12	0.05	0.09	0.08	0.01
DAY 21	0.57	0.14	0.06	0.11	0.09	0.03

3) and subsequent stable adsorption parameters suggest a robust protective mechanism suitable for practical applications requiring long-term corrosion protection.

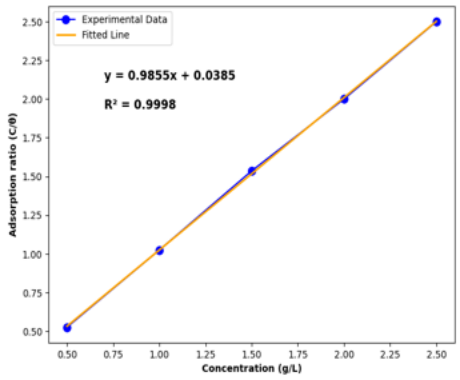

Figure 15: Graph of Langmuir isotherm on Day 3

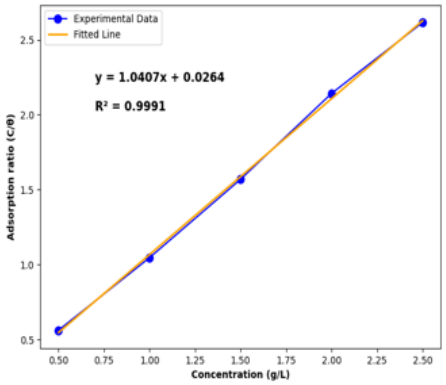

Figure 16: Graph of Langmuir isotherm on Day 6

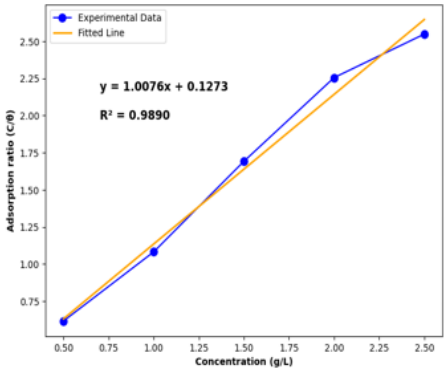

Figure 17: Graph of Langmuir isotherm on Day 9

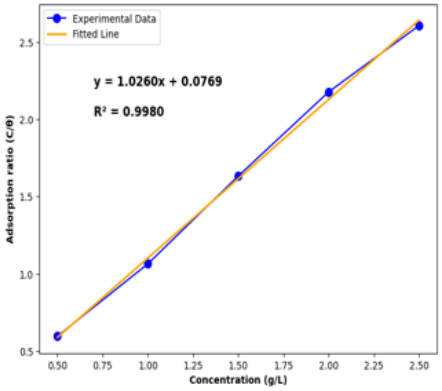

Figure 18: Graph of Langmuir isotherm on Day 12

Table 6: Corrosion rates of AISI 1055 carbon steel in NaCl with Jatropha tanjorensis extract

Time	CR_1 (mm/yr)	CR_2 (mm/yr)	CR_3 (mm/yr)	CR_4 (mm/yr)	CR_5 (mm/yr)	CR_6 (mm/yr)
DAY 3	16.661	0.775	0.387	0.387	0.000	0.000
DAY 6	8.718	0.969	0.387	0.387	0.581	0.387
DAY 9	6.070	0.904	0.258	0.258	0.387	0.129
DAY 12	4.747	0.775	0.291	0.387	0.387	0.194
DAY 15	4.107	0.775	0.310	0.465	0.465	0.078
DAY 18	3.552	0.775	0.323	0.581	0.517	0.129
DAY 21	3.155	0.775	0.332	0.609	0.498	0.166

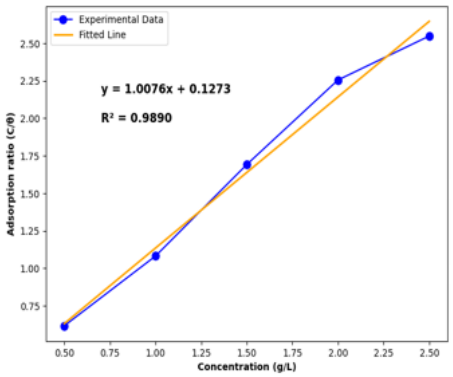

Figure 19: Graph of Langmuir isotherm on Day 15

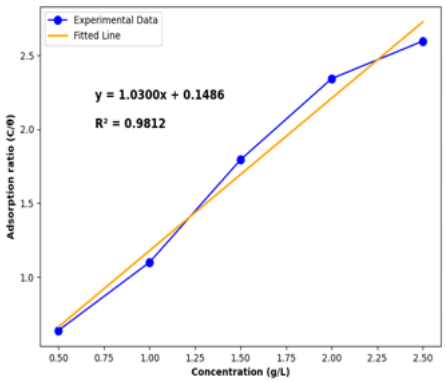

Figure 20: Graph of Langmuir isotherm on Day 18

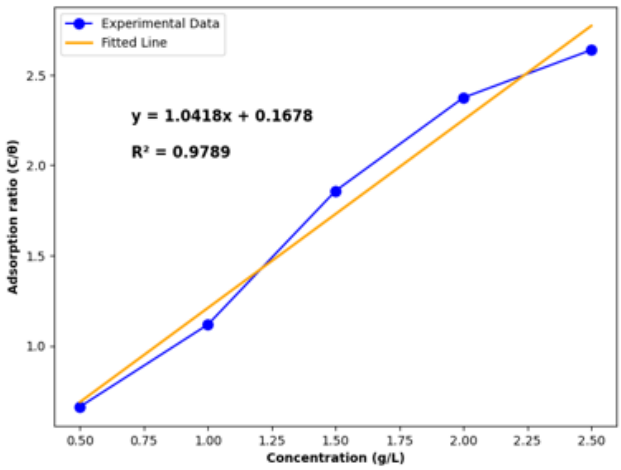

Figure 21: Graph of weight loss against time for uninhibited and inhibited AISI 1055 steel in NaCl

3.5 Scanning Electron Microscopy (SEM) Analysis of a Selected Sample

The SEM analysis of a selected AISI 1055 steel sample exposed to hydrochloric acid (HCl) showed clear differences between the unprotected control sample and the sample treated with 2.5g/L of Jatropha tanjorensis as a corrosion inhibitor, as indicated in Figures 22-27. The control sample's surface was severely rough and uneven, covered with irregular pits and grooves that pointed to uniform corrosion, where the acid aggressively attacked the steel, causing widespread material loss. Darker spots on the surface also hinted at the start of pitting corrosion, a more localised form of damage that could lead to deeper holes and faster degradation. Without any inhibitor, the steel was fully exposed to the acid, allowing the HCl to react directly with the metal and cause deep corrosion over time. In contrast, the inhibited sample looked much smoother, with only fine, parallel stripes instead of deep pits or grooves. These stripes suggested that the inhibitor formed a protective layer on the steel, acting like a shield to limit the acid's ability to attack the metal [48]. While some roughness and grooves were still visible, the corrosion was significantly reduced, showing that the inhibitor slowed down the metal's breakdown in the acid. The 10,000× magnification was emphasised because it provided the clearest, most detailed view of these surface changes. At this high level of zoom, the fine scratches on the inhibited sample and the deep pits on the control sample were much easier to see and compare than at 8,000× or 9,000×. This higher magnification helped confirm the protective effect of the inhibitor and made it easier to distinguish between the types of corrosion damage on the two samples.

3.6 Energy Dispersive Spectroscopy (EDS) Analysis of a Selected Sample

The EDS analysis shown in Figures 28 and 29 further supports the findings from the SEM images by highlighting the differences in elemental composition between the uninhibited and inhibited samples. The control sample exhibited a noticeable reduction in iron (Fe), with its content decreasing to 80.00% compared to 84.02% in the inhibited sample. This suggests that significant Fe dissolution occurred in the absence of an inhibitor, leading to severe material loss. Additionally, the control sample had a higher chlorine (Cl) content (6.00% compared to 4.26% in the inhibited sample), confirming that chloride ions had aggressively attacked the steel, accelerating its degradation. The inhibited sample retained a higher Fe content, indicating that less metal dissolution occurred, which is consistent with the formation of a protective inhibitor layer. Another notable difference was observed in the zinc (Zn) content, which was higher in the inhibited sample (5.23%) than in the control (1.22%). This could indicate that zinc-related corrosion products were forming as part of the protective layer, contributing to passivation. Additionally, the inhibited sample showed increased levels of copper (Cu) and nickel (Ni), likely due to surface enrichment from selective leaching or adsorption of inhibitor components. On the other hand, the control sample exhibited higher levels of aluminium (Al) and silicon (Si), suggesting that more severe corrosion had occurred, exposing underlying substrate materials. The presence of chromium (Cr) in the control but not in the inhibited sample also suggests different corrosion mechanisms or variations in alloy behaviour in the presence of the inhibitor.

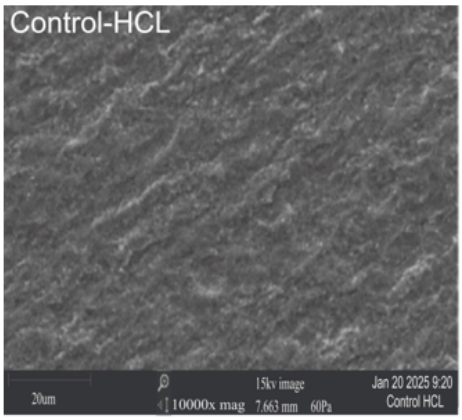

Figure 22: SEM of uninhibited sample (10,000×)

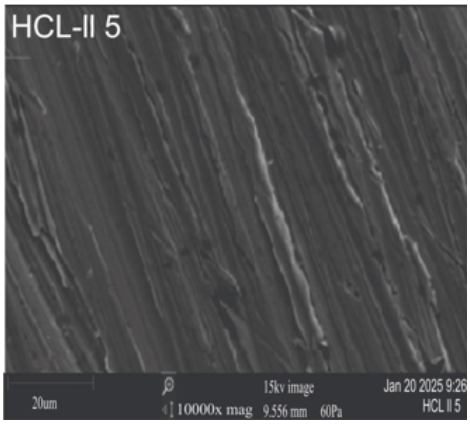

Figure 23: SEM of 2.5g/L inhibited sample (10,000×)

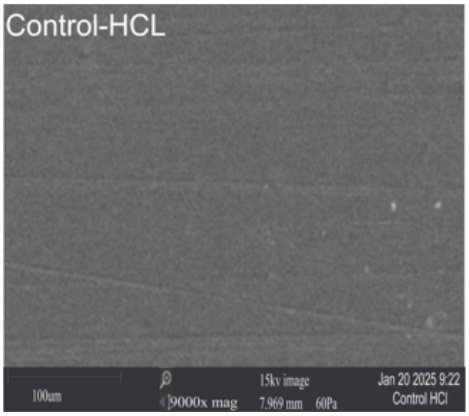

Figure 24: SEM of uninhibited sample (9,000×)

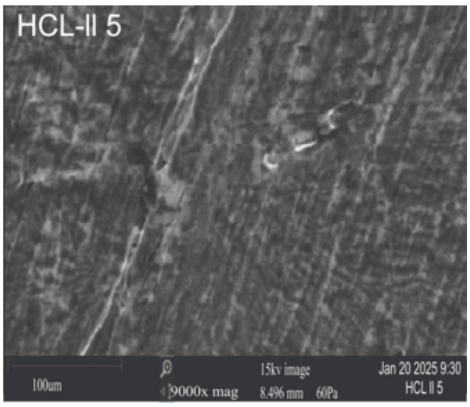

Figure 25: SEM of 2.5g/L inhibited sample (9,000×)

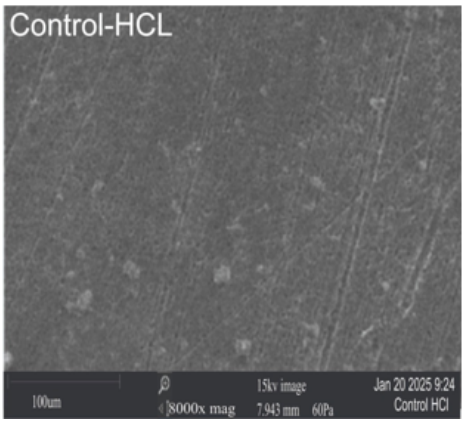

Figure 26: SEM of uninhibited sample (8,000×)

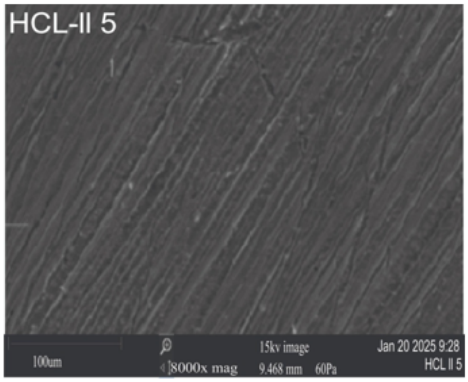

Figure 27: SEM of 2.5g/L inhibited sample (8,000×)

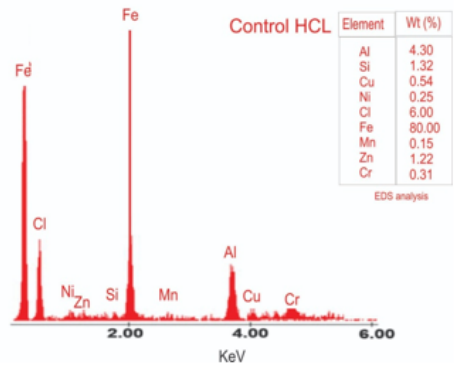

Figure 28: EDS of uninhibited sample

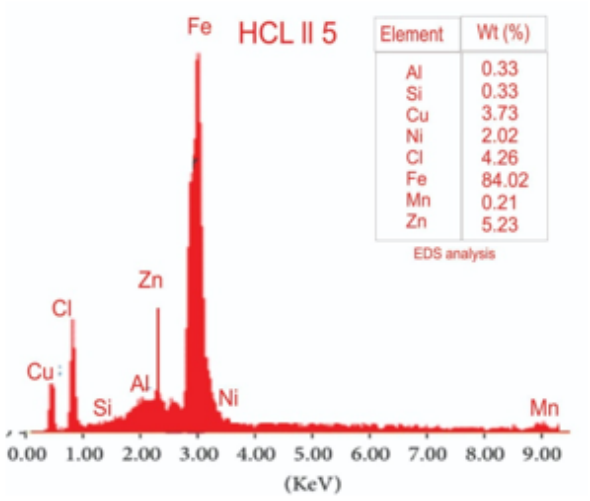

Figure 29: EDS of 2.5g/L inhibited sample

4.0 Conclusions

1. Jatropha tanjorensis extract effectively reduces corrosion rates of AISI 1055 high-carbon steel in both 1 M HCl and 3.5% NaCl environments, with higher concentrations yielding superior protection. At 2.5 g/L, the corrosion rate in HCl dropped to 0.387 mm/yr (Day 21) from the corrosion rate of 2.491 mm/yr for the control, while in NaCl, it decreased to 0.166 mm/yr (Day 21) from 3.155 mm/yr, demonstrating significant inhibition compared to unprotected steel.

2. Inhibition efficiency escalates with increasing extract concentration, achieving remarkable peak values. In NaCl, it reached 100% on Day 3 at 2.0 and 2.5 g/L, stabilizing at 96.48% by Day 21 (2.5 g/L), while in HCl, a maximum of 93.94% was recorded on Day 3 across all concentrations, maintaining 84.46% at 2.5 g/L by Day 21, highlighting robust long-term protective capacity, particularly in saline conditions.

3. Adsorption of Jatropha tanjorensis extract in HCl adheres closely to the Langmuir isotherm, with R^2 values consistently high (e.g., 0.9997 on Day 3, 0.9905 on Day 21), indicating uniform monolayer coverage on the steel surface. In NaCl, adsorption predominantly follows the Langmuir model, with R^2 values peaking at 0.9998 (Day 3) and remaining strong (e.g., 0.9789 on Day 18), confirming a primarily monolayer mechanism.

4. The SEM analysis revealed stark contrasts: the uninhibited sample from HCl solution exhibits severe pitting and rough surfaces, indicative of aggressive corrosion, whereas the 2.5 g/L inhibited sample shows finer stripes and reduced damage, affirming the extract's ability to form a protective film that mitigates acid-induced degradation.

References

[1] S. N. Hong and U. V. T. Nhu, "Multi-objective optimization in turning operation of aisi 1055 steel using dear method," *Tribology in Industry*, vol. 43, no. 1, p. 57, 2021.

[2] S. Mandal, R. Ghosh, S. Kunar, R. Samanta, A. Sinha, and G. Mandal, "Current development of multiphase steel: Alloy design, properties and application," *Journal of the Institution of Engineers (India): Series D*, vol. 105, no. 3, pp. 2023–2038, 2024.

[3] B. L. Bramfitt, "Carbon and alloy steels," in *Mechanical Engineers' Handbook: Materials and Mechanical Design*, 2005, vol. 1, pp. 1–38.

[4] J. Y. Afrifa, E. A. Duodu, N. J. Amoanab, K. Dubik, C. Akasika, and F. Dery, "Impact of electric-arc welding on the mechanical properties of aisi 1055 medium carbon steel with varied gauge diameters," *African Journal of Applied Research*, vol. 9, no. 2, pp. 35–51, 2023.

[5] U. K. Mudali, "Materials for hostile corrosive environments," in *Materials Under Extreme Conditions*, 2017, pp. 91–128.

[6] G. Koch, "Cost of corrosion," in *Trends in Oil and Gas Corrosion Research and Technologies*, 2017, pp. 3–30.

[7] A. R. Prasad, A. Kunyankandy, and A. Joseph, "Corrosion inhibition in oil and gas industry: Economic considerations," in *Corrosion Inhibitors in the Oil and Gas Industry*, 2020, pp. 135–150.

[8] V. U. Okoro, "Corrosion of oil pipeline: A case study on the niger delta region of nigeria," 2023.

[9] F. Smith, F. Brownlie, T. Hodgkiess, A. Toumpis, A. Pearson, and A. M. Galloway, "Effect of salinity on the corrosive wear behaviour of engineering steels in aqueous solutions," *Wear*, vol. 462, p. 203515, 2020.

[10] M. Vakili, P. Koutník, J. Kohout, and Z. Gholami, "Analysis, assessment, and mitigation of stress corrosion cracking in austenitic stainless steels in the oil and gas sector: A review," *Surfaces*, vol. 7, no. 3, pp. 589–642, 2024.

[11] M. A. Ahmed, S. Amin, and A. A. Mohamed, "Current and emerging trends of inorganic, organic and eco-friendly corrosion inhibitors," *RSC Advances*, vol. 14, no. 43, pp. 31 877–31 920, 2024.

[12] M. M. Hanoon, B. S. Mahdi, and A. A. Alamiery, "Green and hybrid corrosion inhibitors: Mechanistic insights and industrial applications," *International Journal of Corrosion and Scale Inhibition*, vol. 14, no. 4, pp. 1716–1784, 2025.

[13] A. A. Al-Amiery, W. N. R. W. Isahak, and W. K. Al-Azzawi, "Corrosion inhibitors: Natural and synthetic organic inhibitors," *Lubricants*, vol. 11, no. 4, p. 174, 2023.

[14] J. Hoshowski, A. Jenkins, and R. P. Pineiro, "The development of environmentally acceptable corrosion inhibitors for sour applications," in *AMPP Corrosion*, 2022, paper D031s031r002.

[15] O. A. Fashae and R. O. Obateru, "Geospatial assessment of surface water pollution and industrial activities in ibadan, nigeria," in *Spatial Modeling and Assessment of Environmental Contaminants: Risk Assessment and Remediation*, 2021, pp. 189–211.

[16] A. O. Stucki, T. S. Barton-Maclaren, Y. Bhuller, J. E. Henriquez, T. R. Henry, C. Hirn, and A. J. Clippinger, "Use of new approach methodologies (nams) to meet regulatory requirements for the assessment of industrial chemicals and pesticides for effects on human health," *Frontiers in Toxicology*, vol. 4, p. 964553, 2022.

[17] A. Zakeri, J. Narenkumar, M. Arthanareeswari, and M. Sundaravadivelu, "Plant extracts as sustainable and green corrosion inhibitors for protection of ferrous metals in corrosive media: A mini review," *Corrosion Communications*, vol. 5, pp. 25–38, 2022.

[18] D. Amaechi, C. Obioha, O. Ugochukwu, and S. Eze, "Phytochemical screening, anti-obesity and hepatoprotective activities of ethanol leaf extract of jatropha tanjorensis in wistar rats," *Asian Journal of Applied Chemistry Research*, vol. 12, no. 4, pp. 20–26, 2022.

Table 7: Inhibition efficiency variation with exposure time

Time	$I.E_1$ (%)	$I.E_2$ (%)	$I.E_3$ (%)	$I.E_4$ (%)	$I.E_5$ (%)
DAY 3	90.70	95.35	97.68	97.68	97.68
DAY 6	86.67	91.11	95.56	95.56	93.34
DAY 9	85.11	89.36	91.48	93.62	95.75
DAY 12	85.72	87.76	91.85	91.85	95.91
DAY 15	84.90	86.80	88.68	90.58	96.23
DAY 18	83.64	85.44	87.27	89.10	96.37
DAY 21	82.44	84.22	85.96	87.73	96.48

[19] N. Bhardwaj, N. Kumar, S. Sharma, H. Lgaz, and R. Salghi, "Phytochemicals as steel corrosion inhibitor: An insight into mechanism," *Corrosion Reviews*, vol. 39, no. 1, pp. 27–41, 2021.

[20] R. Haldhar, D. Prasad, A. Saxena, and A. Kumar, "Corrosion inhibitors: Industrial applications and commercialization," in *Sustainable Corrosion Inhibitors II*, 2021, pp. 219–235.

[21] W. E. Sawyer, T. Ogunmoyole, and T. L. Olatunji, "Threats and conservation strategies of common edible vegetables that possess pharmacological potentials in nigeria," in *Herbal Medicine Phytochemistry*, 2023, pp. 1–35.

[22] K. I. Ijoma and V. I. E. Ajiwe, "Jatropha tanjorensis: A flora of southeast nigeria," *Makara Journal of Science*, vol. 26, no. 2, pp. 120–127, 2022.

[23] T. Sithuba, O. Makanjuola, and E. E. Ebenso, "Corrosion inhibitory potential of selected flavonoid derivatives," *Results in Engineering*, vol. 16, p. 100694, 2022.

[24] P. N. S. Yadav, S. Kumar, and G. Prasad, "Role of hydroxyl group in the inhibitive action of benzoic acid toward corrosion of aluminum in nitric acid," *Corrosion*, vol. 55, no. 10, pp. 937–941, 1999.

[25] J. Feng, X. Wang, Z. Li, and Y. Zhang, "Enhanced removal performance of zero-valent iron towards heavy metal ions by assembling fe-tannin coating," *Journal of Environmental Management*, vol. 319, p. 115619, 2022.

[26] S. M. A. Hosseini, A. Azimi, and T. Shahrabi, "Electrochemical and quantum chemical studies of aromatic amines on the steel corrosion in acid solution," *Corrosion*, vol. 68, no. 7, pp. 600–609, 2012.

[27] R. Kaur, P. Singh, and A. Sharma, "Industrial and environmental applications of plant-derived saponins," *Journal of Plant Growth Regulation*, vol. 43, no. 9, pp. 3012–3026, 2024.

[28] M. Tan, Y. Wang, and X. Liu, "Study on extraction, isolation, and biological activity of saponins from quinoa bran," *Journal of Food Processing and Preservation*, vol. 46, no. 12, p. e17155, 2022.

[29] N. Chaachouay, O. Benkhnigue, and L. Zidane, "Alkaloids: A suitable precursor for nanomaterials synthesis," in *Secondary Metabolites Based Green Synthesis of Nanomaterials and Their Applications*, 2023, pp. 23–48.

[30] M. Shukla, "Synergism in anticorrosive phenomenon of phytochemicals/plant extracts," in *Phytochemistry in Corrosion Science*, 2024, pp. 514–530.

[31] D. S. Chauhan, M. A. Quraishi, and K. R. Ansari, "Molecular structural aspects of organic corrosion inhibitors," *Journal of Molecular Structure*, vol. 1227, p. 129374, 2021.

[32] A. Kokalj, "Corrosion inhibitors: Physisorbed or chemisorbed?" *Corrosion Science*, vol. 196, p. 109939, 2022.

[33] I. B. Obot, N. O. Obi-Egbedi, and S. A. Umoren, "Adsorption characteristics and corrosion inhibitive properties of clotrimazole for aluminium corrosion in hydrochloric acid," *International Journal of Electrochemical Science*, vol. 4, no. 6, pp. 863–877, 2009.

[34] A. A. Rahim and J. Kassim, "Recent development of vegetal tannins in corrosion protection of iron and steel," *Recent Patents on Materials Science*, vol. 1, no. 3, pp. 223–231, 2008.

[35] M. Musah, A. Osman, and A. Ibrahim, "Adsorption kinetics and isotherm models: A review," *Current Journal of Applied Science and Technology*, vol. 41, no. 20, pp. 20–26, 2022.

[36] N. Benzbiria, A. Djedouani, M. Boudalia, and Y. Hamlaoui, "Coupling of experimental and theoretical studies to apprehend the action of benzodiazepine derivative as a corrosion inhibitor for carbon steel in acid medium," *Journal of Molecular Structure*, vol. 1281, p. 135139, 2023.

[37] F. R. Agus and Y. B. S. Manik, "Effect of nacl activator concentration on iodine adsorption of pet-based activated carbon," *Jurnal Sains dan Teknologi*, vol. 13, no. 2, pp. 250–257, 2024.

[38] S. Wan, H. Wang, Y. Li, and D. Zhang, "Anti-corrosion mechanism of parsley extract and synergistic iodide for mild steel corrosion in sulfuric acid solution," *Frontiers in Bioengineering and Biotechnology*, vol. 9, p. 815953, 2021.

[39] I. A. Abro, A. A. Memon, A. H. Mallah, and S. Memon, "Investigation and evaluation of neem leaves extract as a green inhibitor for corrosion of mild steel in acidic medium," *Proceedings of the Institution of Mechanical Engineers, Part C: Journal of Mechanical Engineering Science*, vol. 235, no. 4, pp. 734–743, 2021.

[40] R. T. Loto and M. M. Solomon, "Application of ginger and grapefruit essential oil extracts on the corrosion inhibition of mild steel in dilute acid media," *Scientific African*, vol. 19, p. e01489, 2023.

[41] N. O. Eddy, P. O. Ameh, and C. E. Gimba, "Experimental and quantum chemical studies of synergistic enhancement of corrosion inhibition efficiency," *Results in Chemistry*, vol. 4, p. 100290, 2022.

[42] F. Atan, M. Abdullah, and N. A. Rahman, "The efficiency of moringa leaf as green material carbon steel corrosion inhibitor," in *Journal of Physics: Conference Series*, vol. 2266, no. 1, 2022, p. 012009.

[43] S. Nikpour, R. Naderi, and M. Mahdavian, "Eriobotrya japonica lindl leaves extract application for effective corrosion mitigation of mild steel in hydrochloric acid solution," *Construction and Building Materials*, vol. 220, pp. 161–176, 2019.

[44] T. Jonsson, J. E. Svensson, and M. Halvarsson, "Microstructural investigation of the hcl-induced corrosion of the austenitic alloy 310s," *Oxidation of Metals*, vol. 81, no. 5–6, pp. 575–596, 2014.

[45] J. Wang, J. Li, and H. Qian, "Enhanced anti-infective efficacy of zno nanoreservoirs through controlled release mechanisms," *ACS Applied Materials and Interfaces*, vol. 9, no. 39, pp. 33 609–33 623, 2017.

[46] P. M. Krishnegowda, T. V. Venkatesha, and P. K. M. Krishnegowda, "Acalypha torta leaf extract as green corrosion inhibitor for mild steel in hydrochloric acid solution," *Industrial and Engineering Chemistry Research*, vol. 52, no. 2, pp. 722–728, 2013.

[47] B. J. Akpan, K. K. Alaneme, and M. O. Bodunrin, "Investigation of hardness, microstructure and anti-corrosion properties of zn–zno composite coating," *Case Studies in Chemical and Environmental Engineering*, vol. 5, p. 100187, 2022.

[48] A. Kadhim, A. A. Al-Amiery, and T. S. Gaaz, "A mini review on corrosion, inhibitors and mechanism types of mild steel inhibition in an acidic environment," *International Journal of Corrosion and Scale Inhibition*, vol. 10, no. 3, pp. 861–884, 2021.